Supporting Information for

Epitaxial facet junction on TiO_2 single crystals for efficient photocatalytic water splitting

Methods

Catalyst preparation. The shape-tailored TiO_2 SCs were prepared using a solvothermal method. The shape-tailored TiO_2 SCs with dominant high-energy {001} polar facets were prepared using a facile solvothermal method. Briefly, HF aqueous solution (0.0, 1.5, 3.0, 4.5, 6.0 and 9.0 mL, respectively, 40 wt.%) and distilled water (15.0, 13.5, 12.0, 10.5, 9.0 and 6.0 mL, respectively) were carefully and slowly dosed into 25-mL tetrabutyl titanate, and magnetically stirred for 0.5 h in a 60-mL Teflon autoclave. Later, the slight yellow precursor was kept at 180°C for 24 h. After cooled to ambient temperature, the white powders were repeatedly washed with ethanol, 0.1 M NaOH aqueous solution and distilled water to remove the surface fluorine, and then dried at 60°C for usage. The polycrystalline TiO_2 particles dominantly exposed by low-energy {101} facets were prepared as reference without HF. TiO_2 SCs were characterized in terms of morphology and structures, and their photochemical properties were evaluated in a three-electrode system either in dark or under UV irradiation.

Characterizations of TiO_2 SCs. The morphology and structure of TiO_2 SCs were characterized by field-emission scanning electron microscope (FE-SEM, SIRION200, FEI Co., the Netherlands), high-resolution transmission electron microscope and selected-area electron diffraction (HRTEM/SAED, JEM-2100, JEOL Co., Japan) and scanning transmission electron microscope (STEM, JEM-ARM200F, JEOL Co., Japan). N_2 adsorption-desorption experiments were conducted at 77 K to examine the Brunauer-Emmett-Teller surface area (BELsorp II mini, BEL Inc., Japan). Before measuring, the TiO_2 samples were degassed in a vacuum at 100 ^oC for 12 h. X-ray diffraction (XRD, X'Pert, PAN analytical BV, the Netherlands) was used to analyze the crystal structure. The diffuse reflectance spectra (DRS) were measured on a UV/Vis spectrophotometer (UV 2550, Shimadzu Co., Japan). The chemical compositions and valance band spectra were characterized by X-ray photoelectron spectroscopy (XPS, PHI 5600, Perkin-Elmer Inc., USA), respectively. A FP-6500 spectrofluorometer (Jasco Co., Japan) was used to record the PL spectra of TiO_2 SCs and TiO_2 PCs. The excitation wavelength was set at 360 nm.

Preparation of TiO_2 photoelectrodes. Deposition of the TiO_2 samples onto the commercial ITO glass to fabricate electrochemical and photo-electrochemical electrodes was performed using the facile method reported previously. Briefly, the commercial ITO glass used as substrate were successively cleaned in distilled water, absolute ethanol and isopropanol by ultrasonication for 15 min, then dried at 60 ^oC in vacuum. 5 mg of TiO_2 photocatalyst and 10 μL of Nafion solution (5.0 wt%) were dispersed in 1-mL water/isopropanol mixed solvent (3:1 v/v) by at least 30 min sonication to prepare a homogeneous catalyst suspended colloid. Then, 150 μL of the obtained milk-like viscous catalyst colloid was uniformly spread onto the clean ITO glass of ~6.0 cm^2 (4.0 × 1.5 cm) , by the doctor blade method and then was dried in air to form the working photochemical electrode. After evaporation of ethanol at 120 °C, the samples were heated to 430 °C in a muffle furnace for 2.0 h to completely remove the organic binder and sinter TiO_2 film onto ITO glass. In this process, the ink was dried slowly in open air and the drying conditions were adjusted by trial and error until a uniform catalyst distribution across the electrode surface was obtained. The TiO_2 sample spread uniformly and tightly, indicating that the ITO glass substrate might interact with TiO_2 SCs through physical adsorption, electrostatic binding or charge transfer interaction, and prevent their

severe aggregation. The prepared electrode had a ~0.30 mg TiO_2 dosage (0.05 mg/cm^2 × 6 cm^2) on the ITO glass support, and was stable for the electrochemical and photo-electrochemical measurements under the given conditions.

Electrochemical and photo-electrochemical measurements. All electrochemical and photo-electrochemical properties of TiO_2 samples were measured in a conventional three-electrode measuring system, with the TiO_2 coated ITO glass as the working electrode, platinum sheet as the counter electrode and standard calomel electrode (SCE) as the reference electrode, by using a commercial electrochemical workstation (CHI 760D, CH Instrument, China). Electrochemical impedance spectroscopy of different TiO_2 samples was measured by applying an AC voltage amplitude of 5 mV within a frequency range from 10^5 to 10^{-2} Hz in 0.1 M Na_2SO_4 aqueous solution, with different external potentials and UV illumination.

The photochemical properties were evaluated by the short-circuit photocurrent, the linear sweep voltammogram and the cyclic voltammetry with 0.1 M Na_2SO_4 aqueous solution under UV irradiation (200-400 nm) in a three-electrode system using a computer-controlled potentiostat (CHI 760D, CH Instrument, China). In the tests, TiO_2 samples or commercial ITO glass was used as the working electrode, platinum sheet as the counter electrode and standard calomel electrode (SCE) as the reference electrode (Scheme S1). The light source was a 350 W Xe arc lamp (PLS-SXE350, Beijing Trust Tech Co., China), with a 10 cm infrared water filter and a Pyrex filter ($\lambda >$ 200 nm). In the transition photocurrent tests, the pulse photocurrent with ON/OFF cycles was measured at an applied potential of +0.3 V versus SCE under UV irradiation or in dark. The working electrode was cycled at least 15 times before electrochemical data were recorded, then a continuous or chopped UV irradiation was maintained to activate TiO_2 samples and generate photo-carriers.

Water splitting test. Photochemical H_2 evolution test was carried out on Pt-loaded TiO_2 in a Pyrex reaction cell with gas circulation and evacuation system. A 300-W Xe lamp (PLS-SXE300/300UV, Trusttech Co., China) covered with a water-cooled quartz jacket was used as light source. TiO_2 sample (0.2 g) was suspended in a mixed solution of H_2O (80 mL) and CH_3OH (20 mL). Pt (0.5~3.0 wt%) was deposited onto TiO_2 from $H_2PtCl_6 \cdot 6H_2O$ under UV irradiation (15 min). H_2 amount was in-situ measured using on-line gas chromatography (GC7890, TCD, molecular sieve 5 Å, N_2 carrier, Shanghai Techcomp Co., China).

DFT studies. The first-principles calculations were performed using the DMol package. All calculations were all-electron ones with scalar relativistic corrections. The exchange-correlation interaction was treated by the Perdew-Burke-Ernzerhof (PBE) functional generalized gradient approximation. The basis set consisted of the double numerical atomic orbitals augmented by polarization functions. Along the *b* axis, the periodic boundary condition was applied. The real-space global cutoff radii were chosen to be 4.3 Å, while the Monkhorst-Pack 1×5×1k-points were used for geometry optimization, total energy, and band structure calculations to sample the Brillouin zone. As for the self-consistent electronic structure calculations, the convergence criterions on the energy and electron density are set to be 10^{-6} Hartree (1 Hartree = 1 atomic unit = 27.21 eV). Geometry optimizations are performed with convergence criteria of 2×10^{-3} Hartree/Å on the gradient, 5×10^{-3} Å on the displacement, and 1×10^{-5} Hartree on the energy. To neglect their neighboring interaction, the distance between the neighboring unit cells is larger than 15.0 Å. The calculated crystal parameters of the unit cell of the bulk anatase TiO_2 are a = 3.785 Å and c = 9.486 Å. The {001} facets expose two-fold coordinated, bridging O between two Ti atoms, with Ti-O-Ti angles of 156° together with uncapped, penta-coordinated Ti ions (Ti_{5c}). The {001} anatase contains 5-fold coordinated Ti atoms (Ti_{5c}) each with O_{2c} and O_{3c} on the surface. The {101} facet, which is the most stable and abundant surface in the equilibrium shape of the anatase TiO_2 nanocrystals for reduction reactions, exhibits a saw tooth-like corrugation with Ti_{5c}, Ti_{6c}, O_{2c} and O_{3c} on the surface.

In previous investigations, the band edge positions (E_{CBM} and E_{VBM}) of the isolated TiO_2 {001} and {101} surfaces using slab models were determined according to the method of

Toroker[14]. By performing calculations for the bulk anatase TiO_2 using the PBE and HSE06 functionals, we verified that the band gap center (BGC), denoted E_{BGC}, is insensitive to the choice of the exchange-correlation functional. Thus, the less computationally expensive PBE functional was adopted in our DFT calculations to obtain E_{BGC}. Besides, the band gap calculated using the HSE06 functional was directly comparable to the experimental measurements. The band alignment was determined according to the calculated DOS results as shown in Fig. 4b. The VBM and CBM energy levels could be reliably determined by $E_{VBM} = E_{BGC}-1/2E_g$ and $E_{CBM} = E_{BGC}+1/2E_g$, where E_{BGC} is the BGC position calculated using the PBE functional and E_g is set to be the experimental measured band gaps of 3.18 and 3.22 eV for TiO_2 (001) and (101) surfaces, respectively. Then, the VBM and CBM energy levels of the isolated {001} and {101} facets could be readily aligned relative to their vacuum levels, which are set to zero.

Table S1 Main morphological and structural properties and their photochemical water splitting activities of the TiO_2 samples prepared with different F/Ti molar ratios in the solvothermal process.

F/Ti ratio	HF dosage (mL)	Mean particle size (nm)[a]	Specific surface area ($m^2\ g^{-1}$)[b]	Crystal phase	{001} percent (%)[c]	{001}/{101} exposed ratio[d]	Relative crystallinity[e]	Activity ($\mu mol\ h^{-1}\ g^{-1}$)[f]	Specific activity ($\mu mol\ h^{-1}\ m^{-2}$)[g]
0.00	0.0	~10	168.09	Anatase	9	0.12	1.00	2834.25	16.86
1.15	1.5	~15	95.60	Anatase	37	0.59	1.19	4013.50	41.97
2.30	3.0	~15	95.62	Anatase	48	0.92	1.24	5826.50	60.95
3.45	4.5	~20	93.00	Anatase	56	1.27	1.31	4296.00	46.19
4.60	6.0	~40	62.20	Anatase	74	2.85	1.47	2061.25	33.15
6.90	9.0	~60	37.60	Anatase	84	5.25	1.59	1774.00	47.18

[a] determined by a statistical method from their high-magnification TEM results.

[b] determined by the BET method under typical testing conditions.

[c] determined by a statistical method from their high-magnification SEM and TEM results according to previous studies (Yu et al., J. Am. Chem. Soc. **2014**, 136, 8839-8842; Liu et al., ACS Catal. **2016**, 6, 1097-1108).

[d] calculated with the assumption that only the {001} and {101} facets were co-exposed on the surface of shape-tailored TiO_2 SCs prepared under the given solvothermal conditions.

[e] the relative intensity of diffraction peak from the anatase {101} facets (reference: the TiO_2 sample at F/Ti ratio of 0.00).

[f] date collected from Fig. 3a.

[g] the photochemical H_2 generation on the per m^2 surface of the shape-tailored TiO_2 SCs.

Table S2 Parameters in the simulated results of EIS spectra for TiO_2 SCs with different {001}/{101} exposed ratios.[a]

F/Ti ratio	Testing condition		R_s (Ω cm^{-2})[c]	Q_h ($Ssec^n$ cm^{-2})[c]	n[c]	R_{ct} ($k\Omega$ cm^{-2})[c]	Z_w ($Ssec^{0.5}$ cm^{-2})[c]	C_{ti}/Q_{ti} ($Ssec^n$ cm^{-2})[c]	n[c]	R_{ti}[c]
	Bias (V)	UV								
0.00	OCP[b]	×	84.84	1.61×10^{-2}	0.87	177.07	0.63×10^{-1}	3.10×10^{-5}	/Cti	6.84
	OCP[b]	√	118.44	1.68×10^{-2}	0.83	155.82	0.80×10^{-1}	3.01×10^{-5}	/Cti	7.32
1.15	OCP[b]	×	95.76	1.65×10^{-2}	0.86	189.58	0.84×10^{-1}	2.72×10^{-5}	/Cti	7.90
	OCP[b]	√	116.76	1.74×10^{-2}	0.83	160.27	1.15×10^{-1}	2.95×10^{-5}	/Cti	7.31
2.30	OCP[b]	×	84.98	1.04×10^{-2}	0.83	143.05	0.56×10^{-1}	3.42×10^{-5}	/Cti	5.64
	OCP[b]	√	84.98	1.04×10^{-2}	0.85	143.05	0.56×10^{-1}	3.42×10^{-5}	/Cti	5.64
3.45	OCP[b]	×	89.04	1.47×10^{-2}	0.87	149.18	0.54×10^{-1}	3.06×10^{-5}	/Cti	7.07
	OCP[b]	√	89.04	1.47×10^{-2}	0.87	149.18	0.54×10^{-1}	3.06×10^{-5}	/Cti	7.07
4.60	OCP[b]	×	90.72	1.97×10^{-2}	0.88	134.73	0.35×10^{-1}	2.52×10^{-5}	0.96	11.84
	OCP[b]	√	90.72	1.97×10^{-2}	0.88	134.73	0.35×10^{-1}	2.52×10^{-5}	0.96	11.84
6.90	OCP[b]	×	107.52	2.01×10^{-2}	0.87	89.46	0.42×10^{-1}	2.05×10^{-5}	0.98	7.89
	OCP[b]	√	107.52	2.01×10^{-2}	0.87	89.46	0.42×10^{-1}	2.05×10^{-5}	0.98	7.89
2.30	+0.00	×	88.2	1.74×10^{-2}	0.85	203.53	1.71×10^{-1}	2.81×10^{-5}	/Cti	7.58
	+0.00	√	72.24	1.04×10^{-2}	0.85	185.64	2.21×10^{-1}	3.33×10^{-5}	/Cti	6.03
2.30	+0.10	×	79.8	1.52×10^{-2}	0.86	171.94	1.10×10^{-1}	3.68×10^{-5}	/Cti	6.24
	+0.10	√	72.24	1.20×10^{-2}	0.85	124.15	1.65×10^{-1}	3.87×10^{-5}	/Cti	5.12

2.30	+0.20	×	78.12	1.70×10^{-2}	0.87	154.56	2.24×10^{-1}	3.57×10^{-5}	/Cti	5.94
	+0.20	√	77.28	0.94×10^{-2}	0.88	96.76	3.07×10^{-1}	3.31×10^{-5}	/Cti	6.19
2.30	+0.30	×	42.84	1.68×10^{-2}	0.83	110.96	2.34×10^{-1}	2.20×10^{-5}	/Cti	5.12
	+0.30	√	76.44	1.24×10^{-2}	0.87	45.27	11.62×10^{-1}	3.92×10^{-5}	/Cti	5.13
2.30	+0.40	×	88.2	0.96×10^{-2}	0.90	55.18	7.73×10^{-1}	2.60×10^{-5}	/Cti	7.84
	+0.40	√	80.64	1.47×10^{-2}	0.89	25.87	27.66×10^{-1}	3.67×10^{-5}	/Cti	6.24
2.30	+0.50	×	74.76	1.25×10^{-2}	0.88	41.07	17.32×10^{-1}	3.89×10^{-5}	/Cti	5.14
	+0.50	√	82.32	0.92×10^{-2}	0.90	13.35	22.97×10^{-1}	4.03×10^{-5}	/Cti	5.11

[a] EIS testing conditions: the typical three-electrode system with the TiO_2 coated ITO glass as the working electrode, platinum sheet as the counter electrode and standard calomel electrode (SCE) as the reference electrode, electrochemical workstation (CHI 760D, CH Instrument, China), supporting electrolyte (0.1 M Na_2SO_4 aqueous solution), voltage amplitude (5 mV), frequency range (10^5 ~ 10^{-2} Hz), bias (OCP or +0.00 ~ + 0.50 V/SCE), UV (500 W Xe arc lamp, $\lambda < 420$ nm) and effective anode area (6.0 cm^2).

[b] OCP: open-circuit potential under the given conditions.

[c] The equivalent circuit of the electrochemical and photo-electrochemical testing systems for EIS simulation was adopted from a similar literature (Xiao et al., Electrochem. Commun. **2007**, 9, 2441-2447). R_s: bulk electrolyte resistance. Q_h: electrochemical double-layer capacitance. R_{ct}: charge-transfer resistance. Z_w: Warburg impedance. R_{ti}/Q_{ti} is associated with the conductivity and capacitance of the TiO_2 modified electrodes. The constant phase element (CPE) Q can replace the electrochemical double-layer capacitance at the electrode-electrolyte interface. The impedance of CPE is given by $Q = \frac{1}{Y(j\omega)^n}$, where Y is the admittance magnitude of CPE and n is the exponent related to the phase angle $\varphi = n(\pi/2)$.

Table S3 Averaged Mulliken population (in *electron*) of one Ti atom and two O atoms on the {001} and {101} facets of shape-tailored anatase TiO_2 SCs using the *co-exposed* and *slab* calculation models, comparatively.

	{101} facet		**{001} facet**	
	Co-exposed model	Slab model	Co-exposed model	Slab model
Ti	+1.423	+1.463	+1.385	+1.398
O_1	-0.581	-0.595	-0.676	-0.685
O_2	-0.797	-0.811	-0.701	-0.735
Net population	+0.045	+0.057	+0.008	-0.022

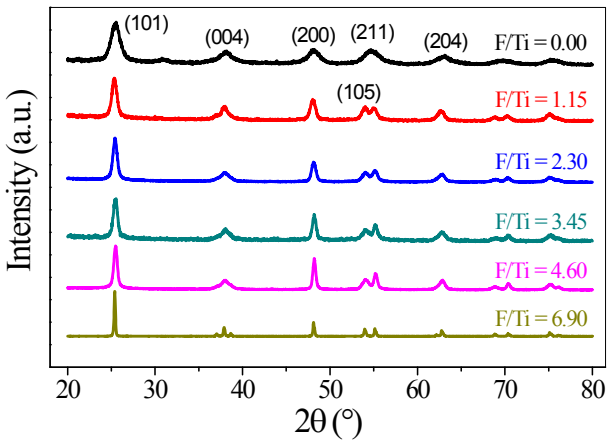

Fig. S1 XRD patterns of the shape-tailored TiO_2 single crystals with different HF dosages (F/Ti = 0.00 ~ 6.90).

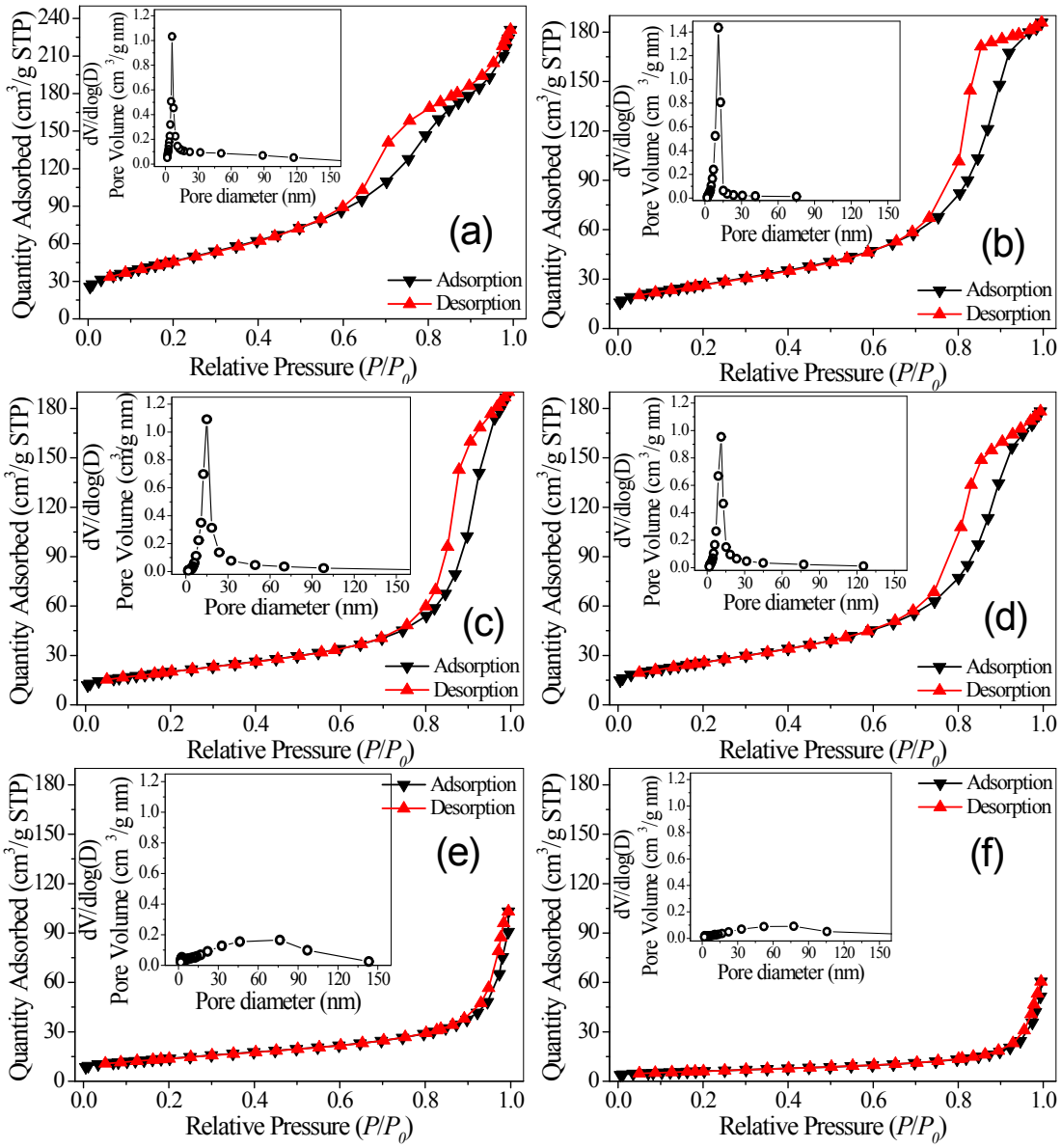

Fig. S2 BET spectra of the shape-tailored TiO_2 single crystals prepared with different HF dosages: F/Ti = 0.00 (a), F/Ti = 1.15 (b), F/Ti = 2.30 (c), F/Ti = 3.45 (d), F/Ti = 4.50 (e) and F/Ti = 6.90 (f).

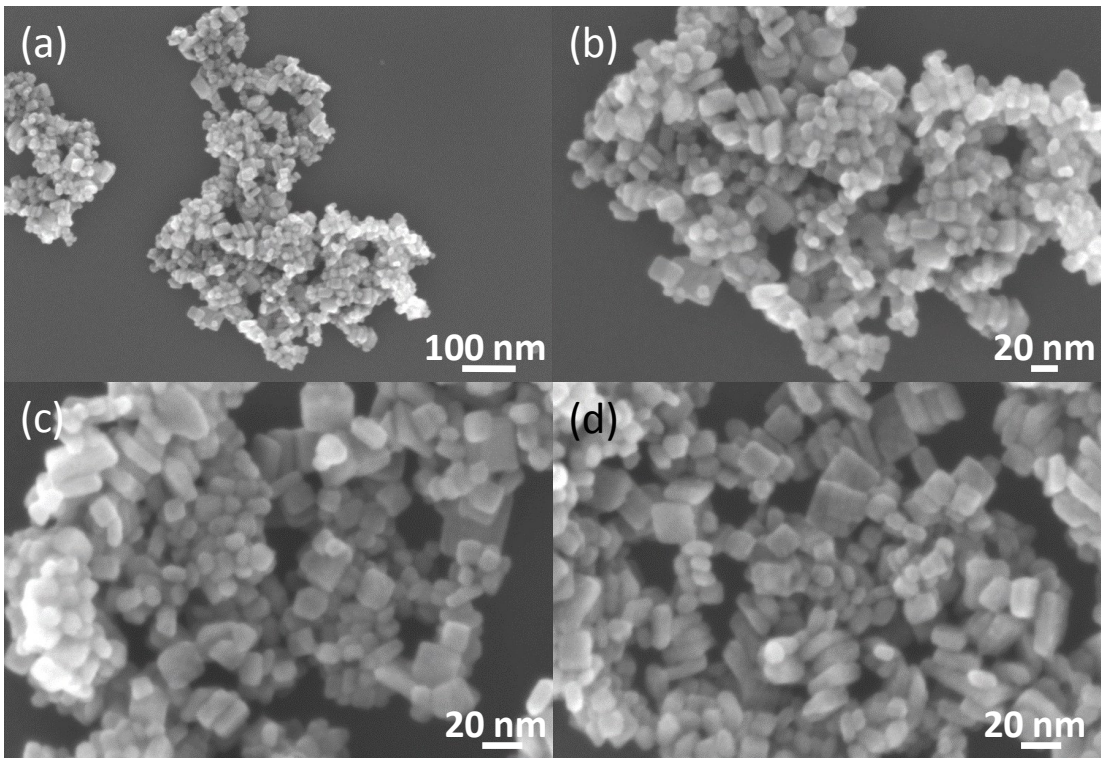

Fig. S3 Typical SEM images of the shape-tailored TiO_2 single crystals prepared with F/Ti = 2.30 at different magnifications (a-d).

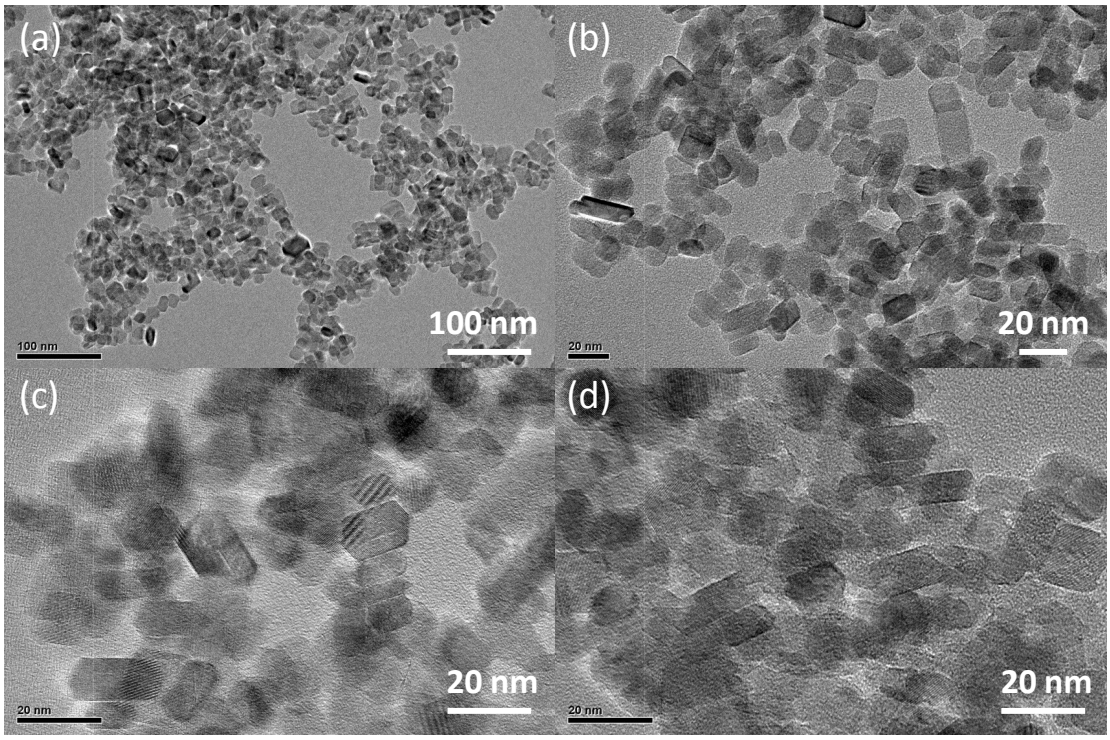

Fig. S4 Typical TEM images of the shape-tailored TiO_2 single crystals prepared with F/Ti = 2.30 at different magnifications (a-d).

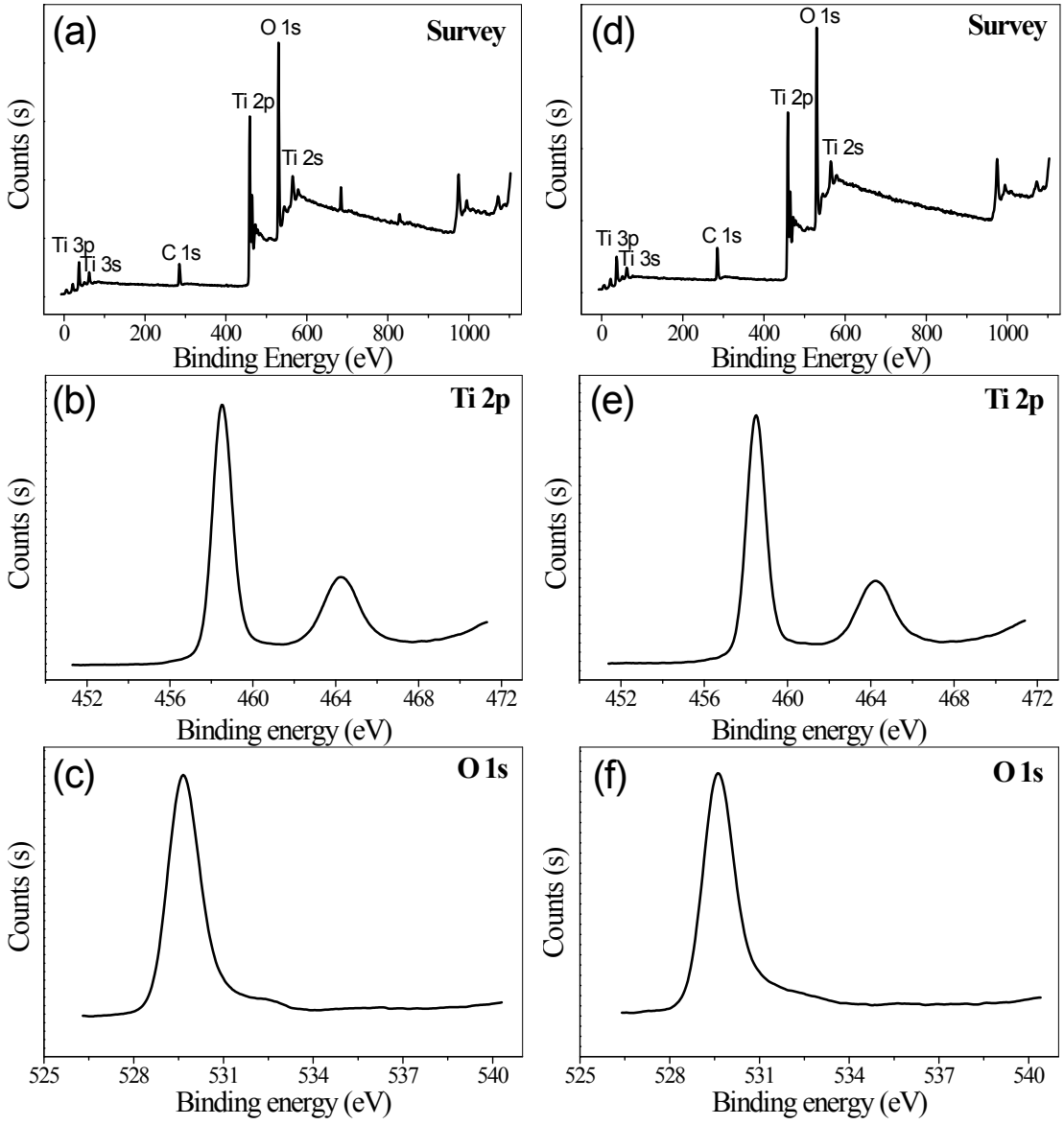

Fig. S5 XPS spectra of the shape-tailored TiO_2-{101}/{001} (F/Ti = 2.30) (a, b and c) and TiO_2-{101} benchmark (F/Ti = 0.00) (d, e and f).

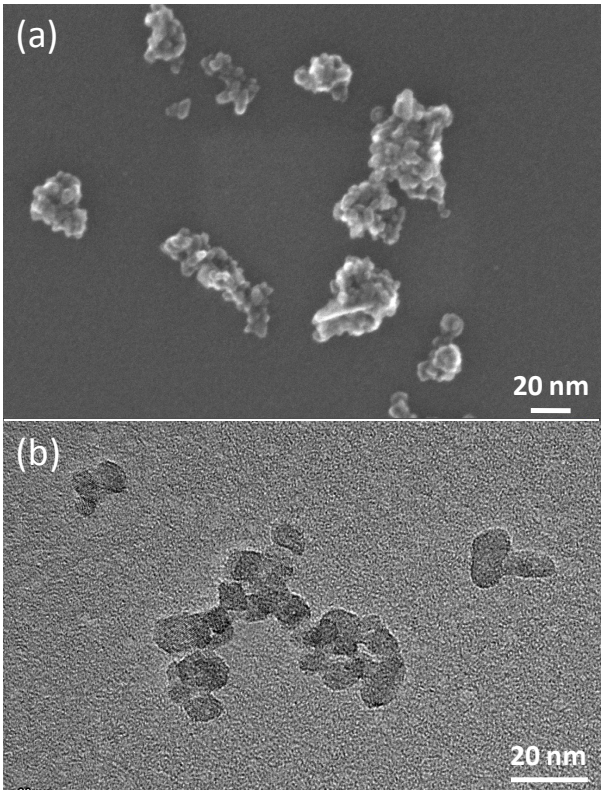

Fig. S6 Typical SEM and TEM images of the TiO_2-{101} benchmark (F/Ti = 0.00).

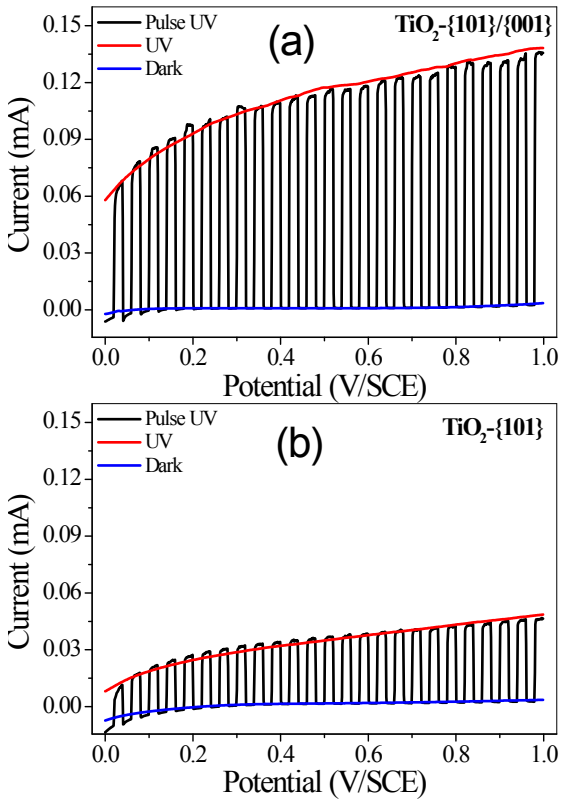

Fig. S7 Linear sweep voltammograms and transient current response to illumination on-off cycles at anodic potential from 0.0 to 1.0 V (V/SCE) at a scan rate of 5 mV s^{-1} with Pt as the counter electrode on TiO_2-{101}/{001} (F/Ti = 2.30) and TiO_2-{101} (F/Ti = 0.00) electrodes.

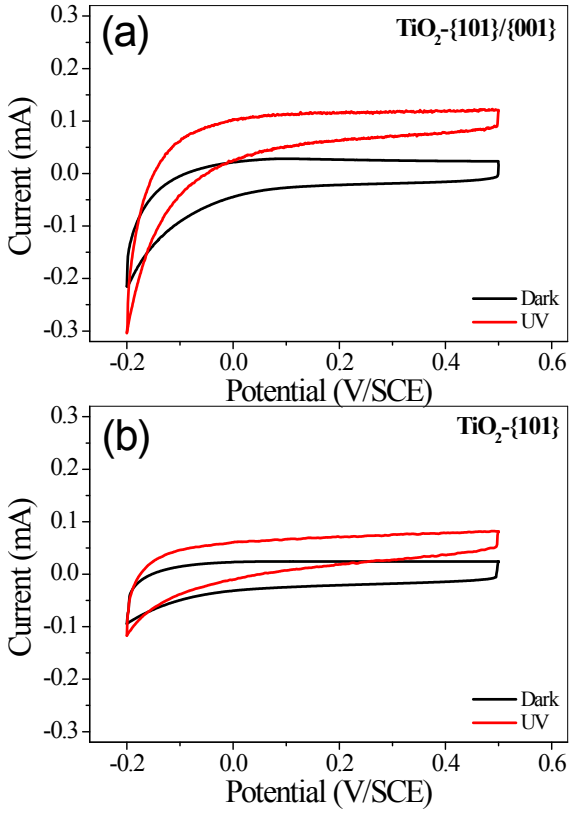

Fig. S8 Cyclic voltammetry from -0.2 to +0.5 V (V/SCE) on the TiO_2-{101}/{001} (F/Ti = 2.30) and TiO_2-{101} (F/Ti = 0.00) electrodes at a scan rate of 50 mV s^{-1} with Pt as the counter electrode in the dark and under UV irradiation.

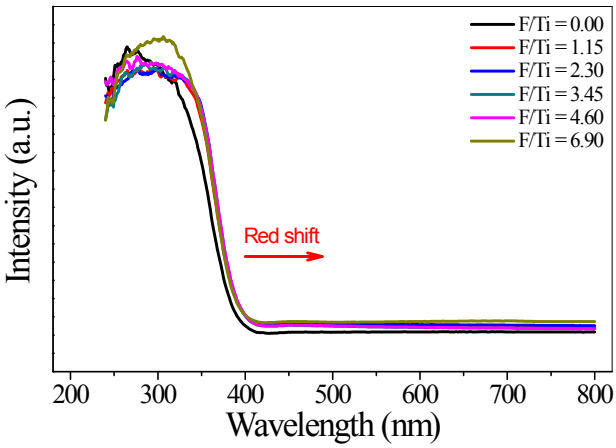

Fig. S9 DRS spectra of the shape-tailored TiO_2 single crystals prepared with different HF dosages (F/Ti = 0.00 ~ 6.90).

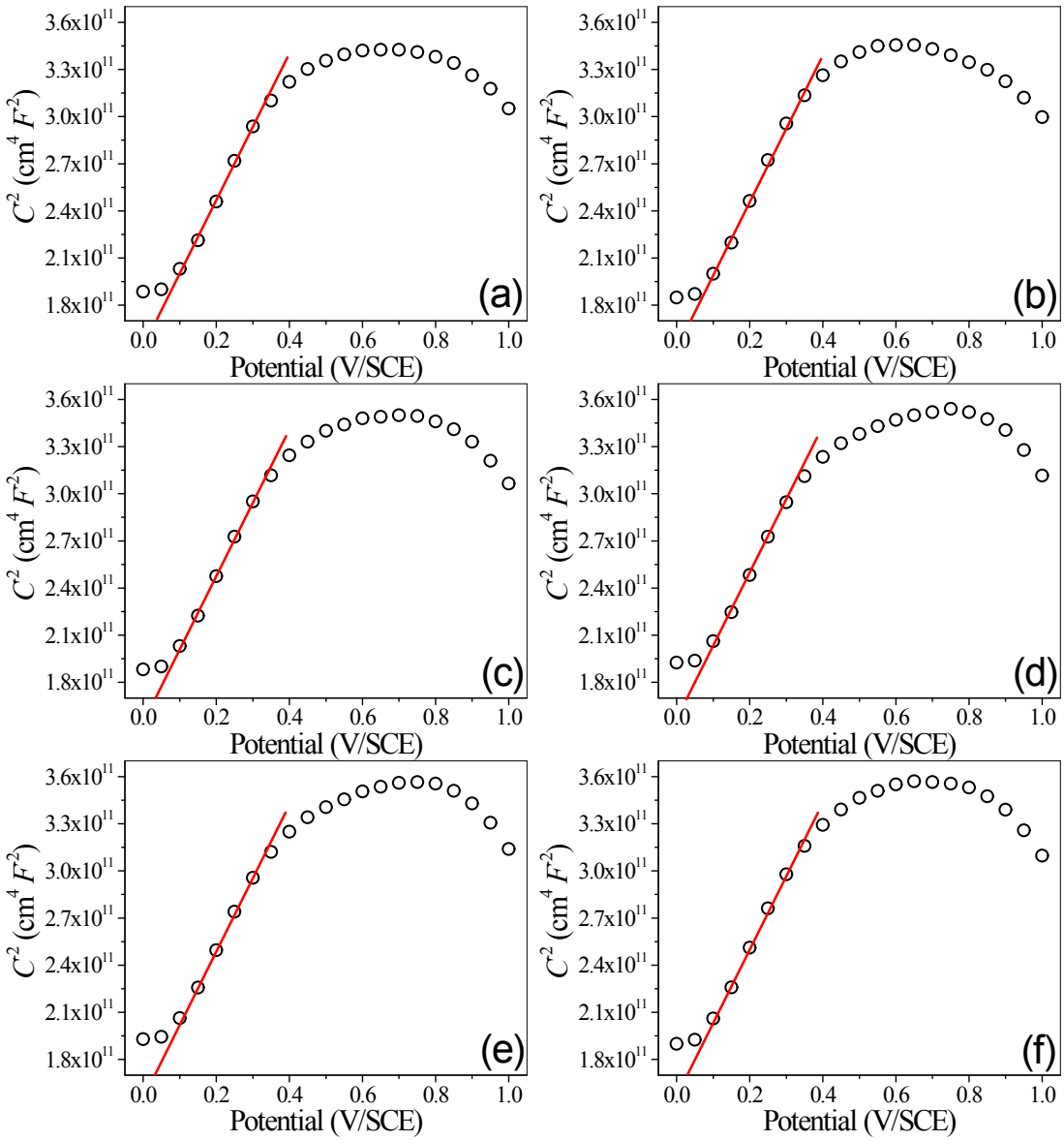

Fig. S10 Mott-Schottky (MS) plots of the shape-tailored TiO_2 single crystals prepared with different HF dosages: F/Ti = 0.00 (a), F/Ti = 1.15 (b), F/Ti = 2.30 (c), F/Ti = 3.45 (d), F/Ti = 4.50 (e) and F/Ti = 6.90 (f). Testing conditions: three-electrode system, electrolyte (0.1 M Na_2SO_4 aqueous solution), frequency (1000 Hz) and voltage (-0.50 to 1.0 V).

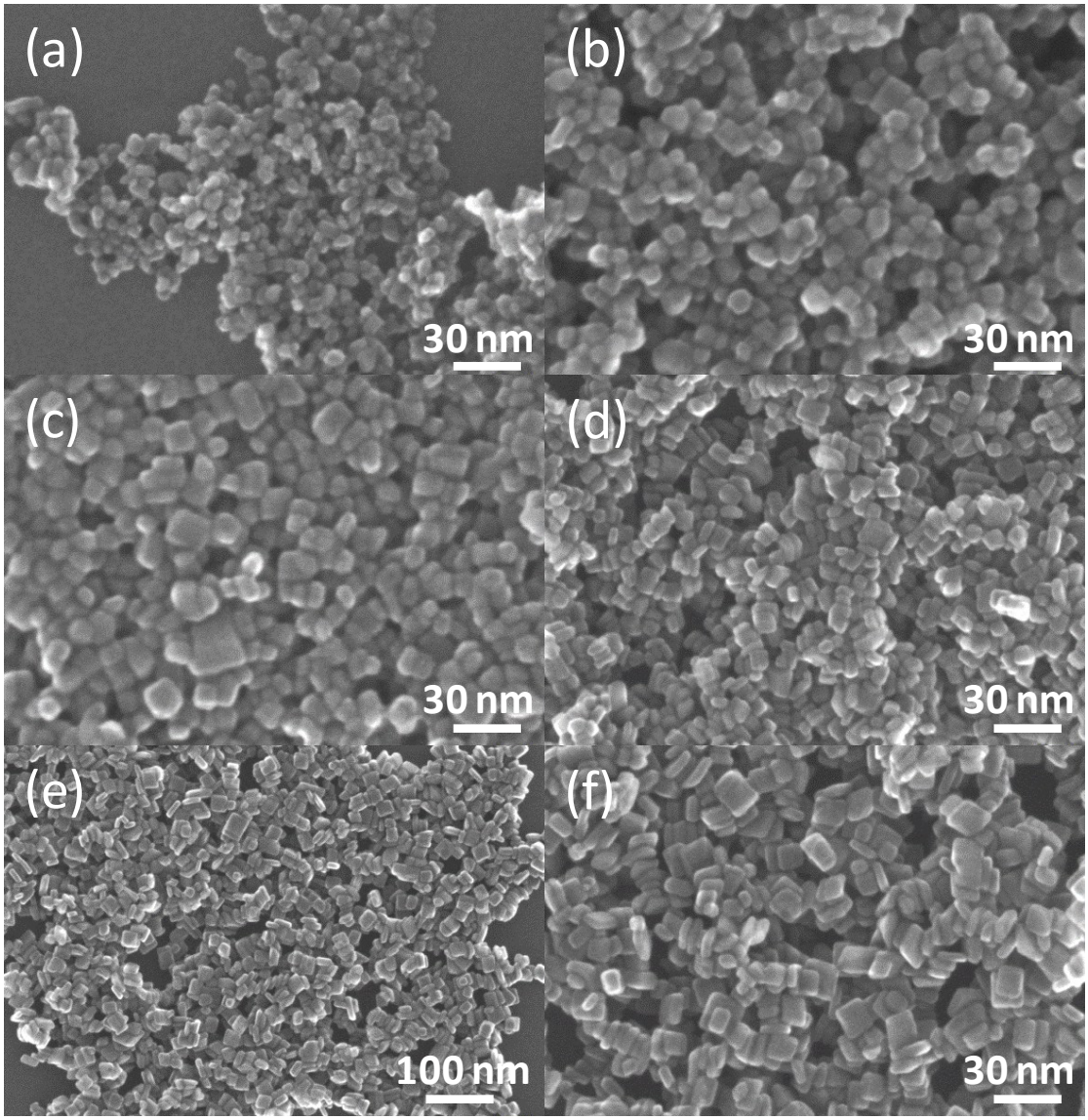

Fig. S11 Typical SEM images of the shape-tailored TiO_2 single crystals prepared with different HF dosages: F/Ti = 0.00 (a), F/Ti = 1.15 (b), F/Ti = 2.30 (c), F/Ti = 3.45 (d) and F/Ti = 4.60 (e, f).

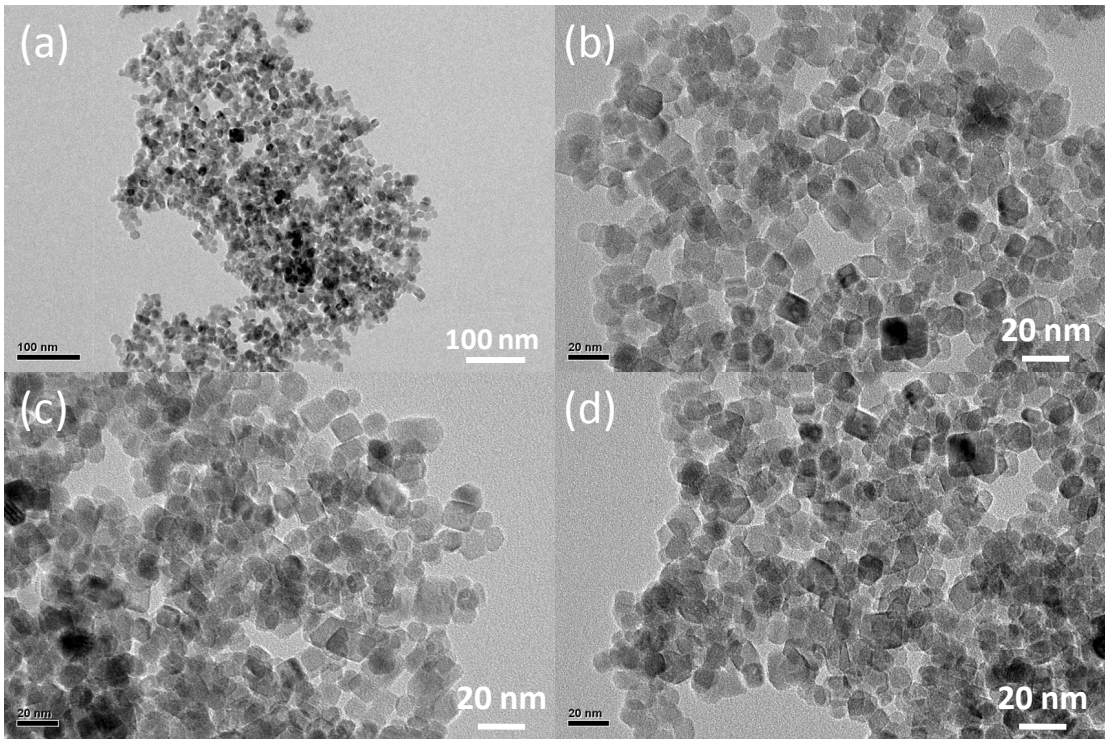

Fig. S12 Typical TEM images of the anatase TiO_2 sample prepared with F/Ti = 1.15 at different magnifications (a-d).

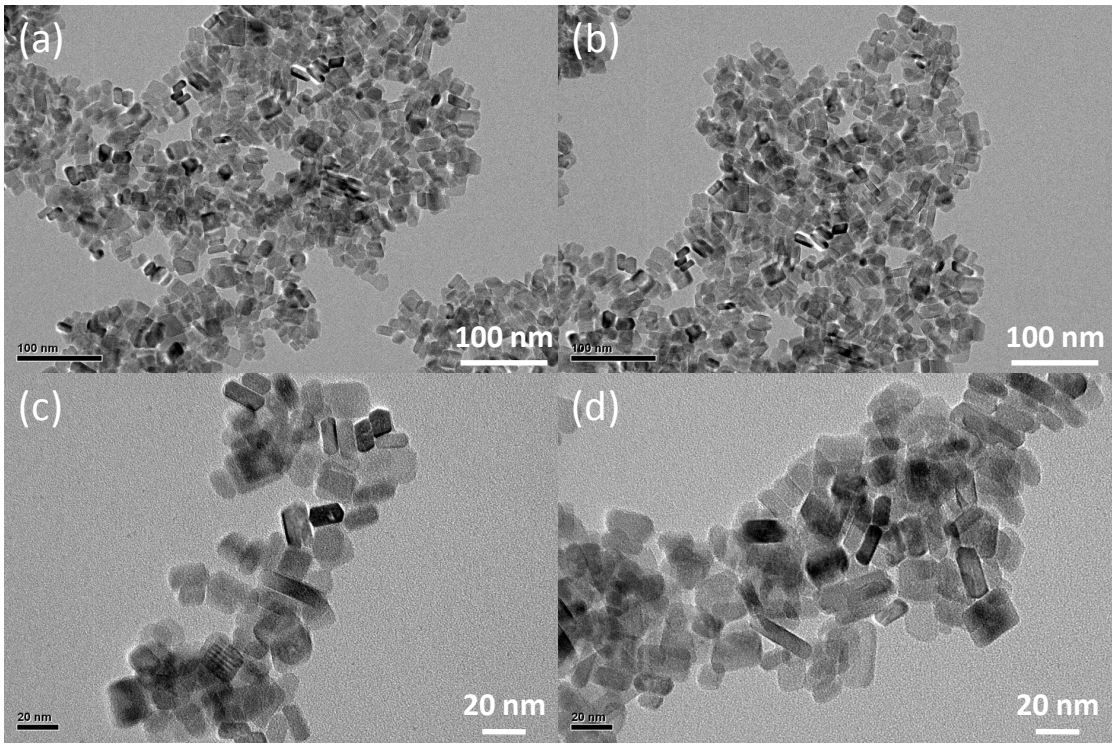

Fig. S13 Typical TEM images of the anatase TiO_2 sample prepared with F/Ti = 3.45 at different magnifications (a-d).

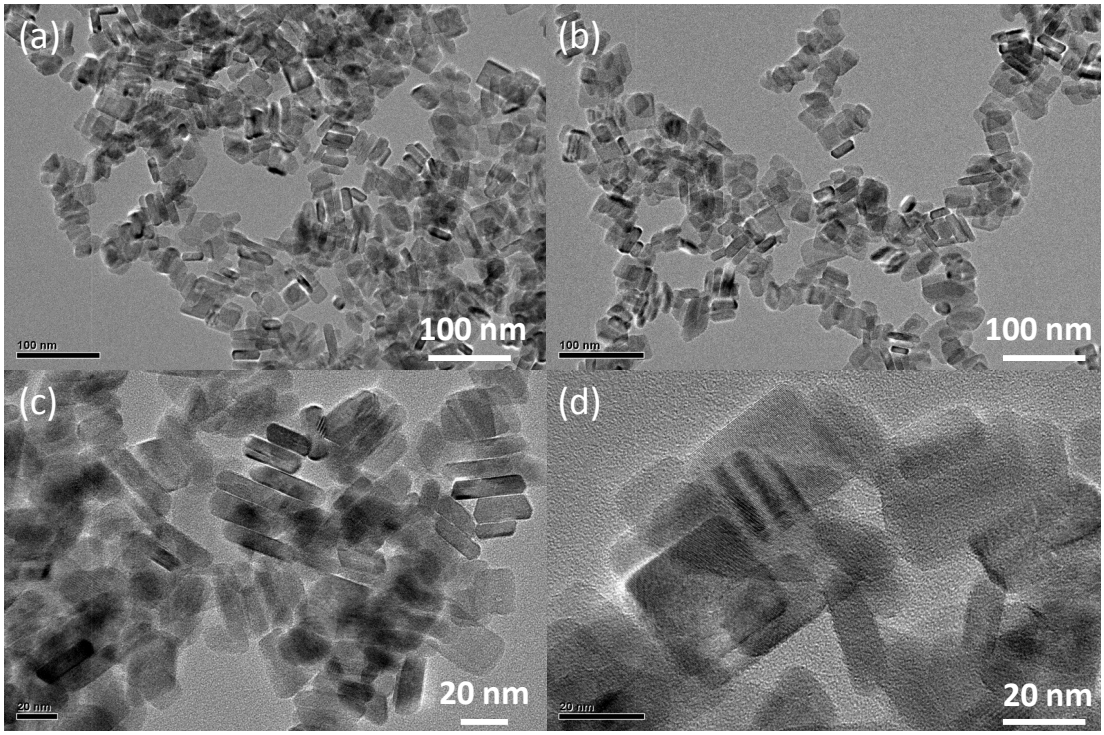

Fig. S14 Typical TEM images of the anatase TiO_2 sample prepared with F/Ti = 4.60 at different magnifications (a-d).

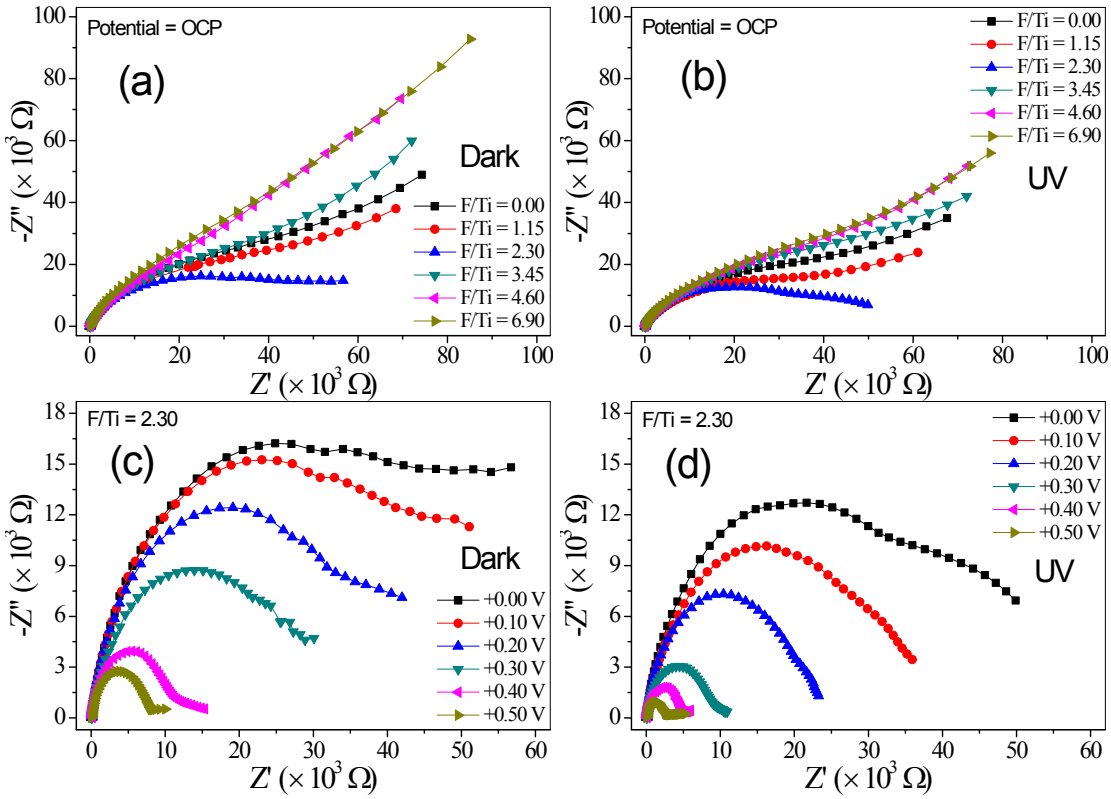

Fig. S15 Electrochemical impedance spectroscopy of TiO_2 samples prepared with different HF dosages (F/Ti = 0.00 ~ 6.90) in dark (a,c) and UV irradiation (b,d) at different anodic bias (V/SCE).

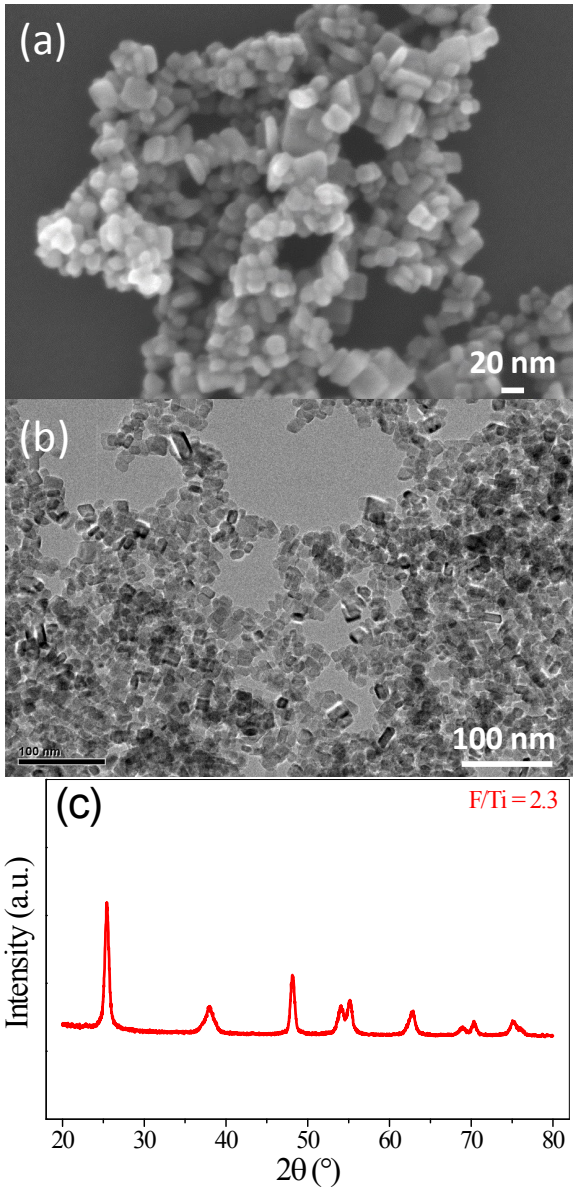

Fig. S16 SEM (a), TEM (b) and XRD patterns (c) of the used TiO_2 single crystals prepared with F/Ti = 2.30 after 5-run cyclic tests for photochemical water splitting.

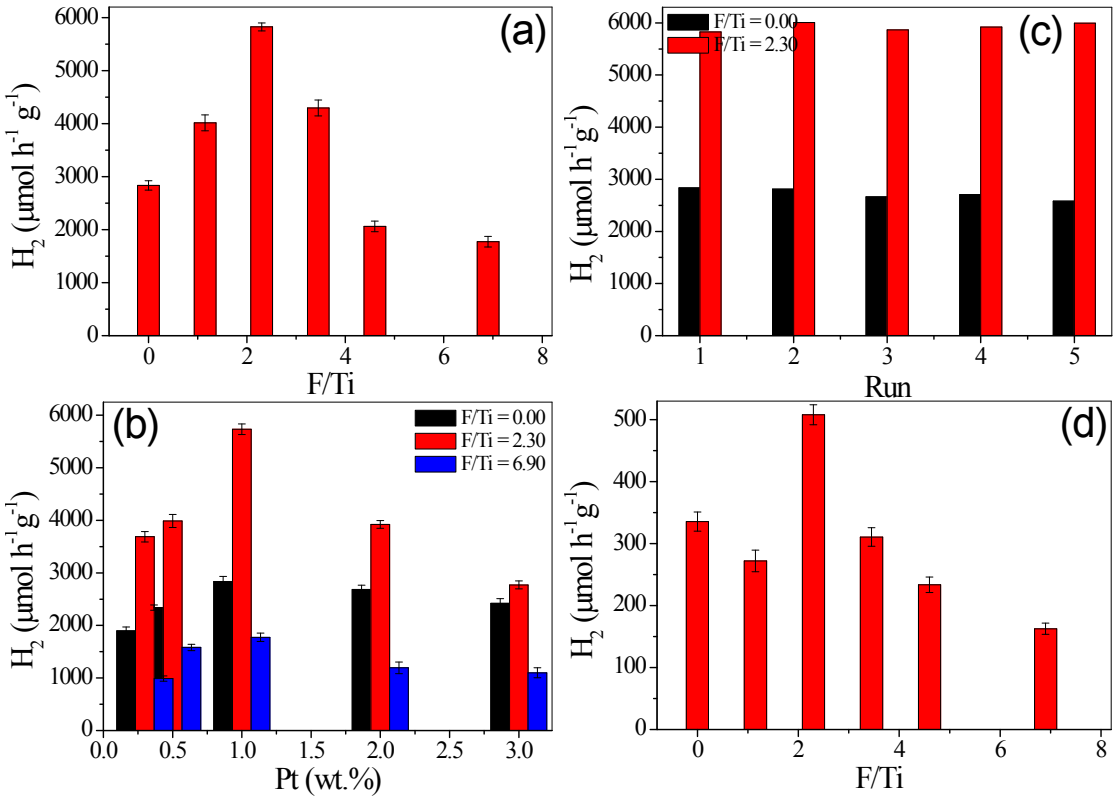

Fig. S17 Photochemical H_2 evolution rates on the TiO_2-{101}/{001} (F/Ti = 1.15 ~ 6.90) and TiO_2-{101} (F/Ti = 0.00) with (a-c) and without Pt cocatalyst (d).

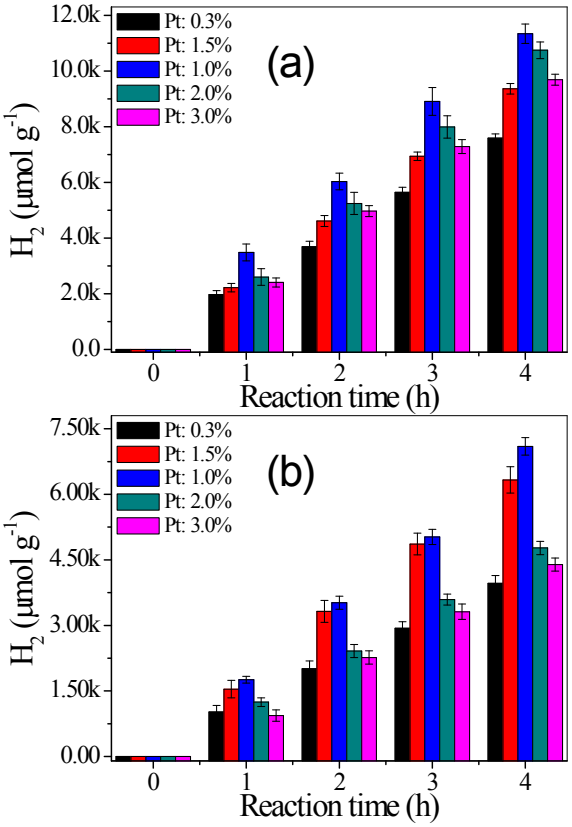

Fig. S18 Photochemical water splitting on TiO_2-{101} (F/Ti = 0.00) (a) and TiO_2-{101}/{001} (F/Ti = 6.90) (b) with Pt cocatalyst at different amounts.

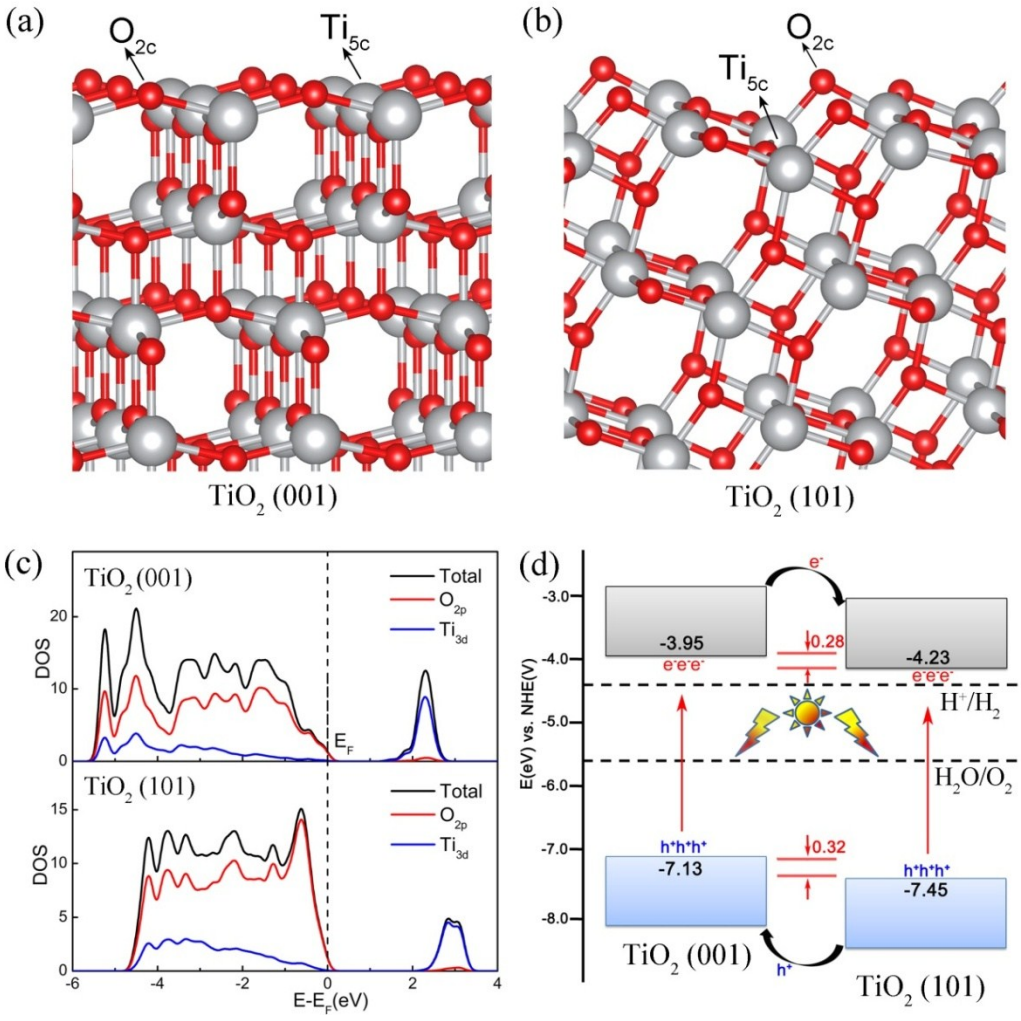

Fig. S19 Schematic illustration of the {001} facet (a), {101} facet (b) of anatase TiO_2 single crystals, calculated density of states (c) and edge alignment between the isolated {001} and {101} facets (d).

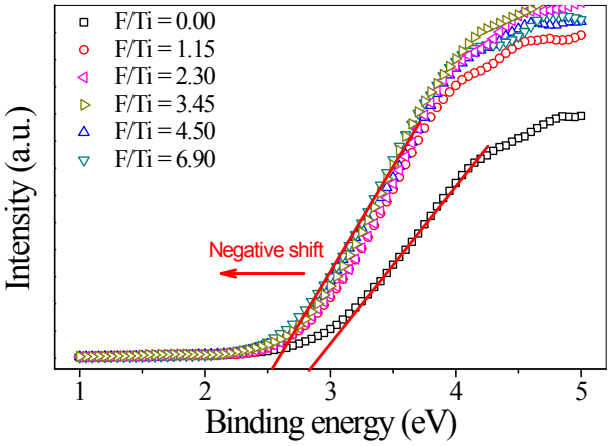

Fig. S20 Valance-band XPS spectra of the shape-tailored TiO_2 single crystals prepared with different HF dosages: F/Ti = 0.00 (a), F/Ti = 1.15 (b), F/Ti = 2.30 (c), F/Ti = 3.45 (d), F/Ti = 4.50 (e) and F/Ti = 6.90 (f).

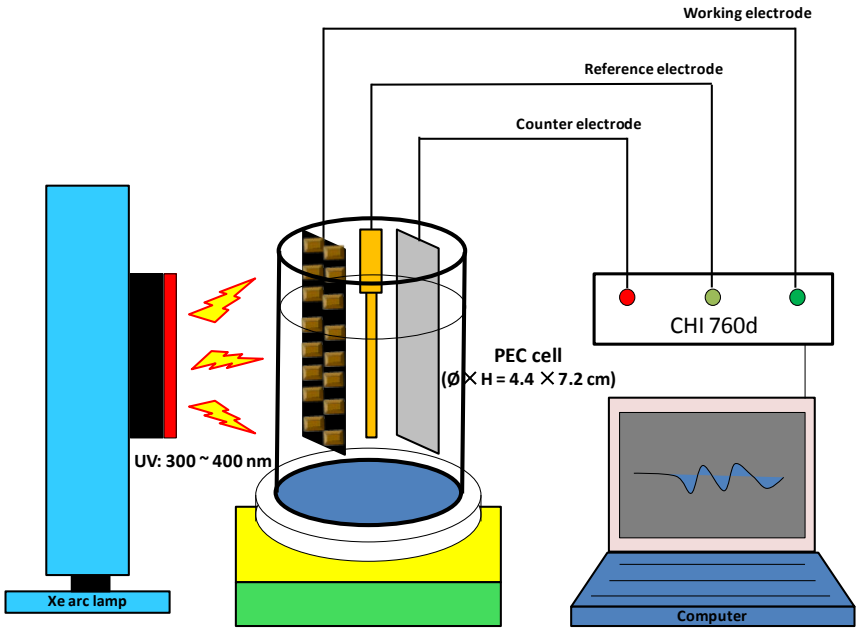

Scheme S1 Schematic diagram of the electrochemical and the photo-electrochemical testing systems.